Carbonate grain-size distribution in hemipelagic sediments from a laser particle sizer

A. Trentesaux, Philippe Recourt, Viviane Bout-roumazeilles, Nicolas
Tribovillard

1 **Carbonate grain-size distribution in hemipelagic sediments from a laser**

2 **particle sizer**

3

4 Trentesaux, A., Recourt, P., Bout-Roumazeilles, V., Tribovillard, N.

5

6 Laboratoire de Sédimentologie et de Géodynamique, UMR 8577, Université des Sciences et

7 Technologies de Lille, SN5, F-59655 Villeneuve d'Ascq Cedex, France

8 e-mail : alain.trentesaux@univ-lille1.fr

9

10 **Abstract**

11   Laser grain-sizer instruments provide the opportunity to study the grain size

12 distribution of sediments across a wide size range in a short time. Automatic

13 Tapez une équation ici.measurements can therefore be made, on a routine basis, for a great

14 number of samples. Oceanic studies have proved the utility of these methods in characterizing

15 both climatic changes and changes in sediment provenances. In addition, carbonate content is

16 estimated either directly by $CaCO_3$ measurement, by visual observations, or by proxies such

17 as sediment color reflectance. Nevertheless, the grain size distribution of the carbonate

18 fraction is still a matter of speculation, and only optical observations can distinguish the

19 nature of each carbonate fraction. Here we present the improvements on a method to study

20 rapidly, with a high resolution, the grain size distribution of the carbonate fraction by use of a

21 laser grain-sizer. We describe the basic methodology and apply it to an example from the

22 Pleistocene of the Northern Atlantic Ocean.

23

24 **Introduction**

25   In paleoceanographic studies, grain size distribution and carbonate content are often

26 examined. The first parameter is derived by a number of methods, each having some

27 advantages and drawbacks. It provides valuable information on the depositional mechanisms

28 (Clemens and Prell 1990; Rea and Hovan 1995; Prins 1997; Kaiho 1999; Wang et al. 1999)

29 and sea-floor currents (Pudsey 1992; Faugères and Stow 1993; McCave et al. 1995a; McCave

30 et al. 1995b; Diekmann and Kuhn 1997; Michels 2000). Carbonate content is usually obtained

31 by chemical digestion, X-ray diffraction, and, more recently, the use of sediment color

32 reflectance as a proxy for carbonate content (Blum 1997; Balsam et al. 1999).

33   In this paper, we discuss a method that facilitates rapid measurement of the two

34   parameters with a good degree of accuracy, including the grain size distribution of the

35   carbonate fraction. The method uses a wide-range laser diffraction size analyzer. A brief

36   application is presented on samples from a Pleistocene climatic transition in Northern Atlantic

37   sediments from an Ocean Drilling Program core. This method offers a good alternative to

38   some classical measurements performed through smearslide observations or differential

39   chemical digestions and microscopic observations (Diekmann and Kuhn 1997).

40

41   **Method**

42   *Measurement Principle*

43   For this study, grain size parameters were determined using a Malvern Mastersizer X

44   apparatus. Other manufacturers exist, and in all cases the instruments use the diffraction of a

45   laser light in a cell filled with the sample in suspension in a dispersant (usually deionized

46   water). The diffraction angle is inversely proportional to the grain size and is measured with a

47   photoelectric cell. A series of algorithms are then used to calculate a grain size distribution

48   curve assuming a spherical shape of the particles. For these instruments, manufacturers

49   indicate that typical accuracy is less than 2% for grain sizes between 900 and 5 μm and

50   decreases to about 6% for finer grain sizes. Manufacturers' reported precision is 2%. The

51   measurement principle is well explained in McCave et al. (1986) and Agrawal et al. (1991).

52   The relative advantages or drawbacks of this technique and other grain-size analyzers

53   have been well documented (McCave and Syvitski 1991; Loizeau et al. 1994; Kench and

54   McLean 1997; Konert and Vandenberghe 1997; Beuselinck et al. 1998). Among the

55   advantages that led us to choose this technique instead of others is the good precision and the

56   rapidity of the measurement, allowing the study of large sample sets. Four lenses are

57   available, depending on the estimated grain size distribution: 45, 100, 300, and 1000 mm,

58   respectively for 0.1 80, 0.5 180, 1.2 600, and 4.0 2000 μm, respectively. The 100 mm lens

59   was selected because it was the most suitable for our tests.

60

61   *Sample Preparation*

62   In the case of a coarse fraction, the sediment can be gently sieved under deionized

63   water. Samples were first put in suspension in deionized water and then gently shaken for two

64   hours to achieve disaggregation. For organic-rich sediments, it might be interesting to use

65   H2O2 to oxidize organic matter and to break up the floccules; this has not been tested in our

66   studies. In contrast to the treatment proposed by Loizeau et al. (1994), sonication was not

67   used to complete the sediment dispersion. Measurements showed that after more than two

68   hours of gentle shaking, the suspended sediment is well disaggregated. Moreover, the use of

69   ultrasonic dispersion has a dramatic effect on some particles containing trapped water

70   inclusions, such as foraminifers or vesicular volcanic glass. Repeated measurements after

71   increasing periods of ultrasonic dispersion clearly demonstrate the disintegration of the

72   foraminifer tests and vesicular glass particles, leading to a decrease in the mean sediment

73   grain size. Broken foraminifer tests can subsequently be observed in residues on smear slides.

74   The suspension is then gently poured into the fluid module of the granulometer, filled

75   with tap water. Tap water was chosen rather than degassed water for reasons of simplicity.

76   The background noise introduced by the degassing water (Loizeau et al. 1994) is nevertheless

77   small and is included in the measured background that is later subtracted from the total

78   measurement. Ultrasonics is used before pouring the sediment in order to decrease the

79   degassing time. The final suspension has a concentration varying from 10"4 to 0.1%

80   (expressed as a relative volume concentration). Measurement begins after two minutes of

81   continuous stirring to allow most of the air bubbles created by the sediment introduction to

82   escape.

83

84   *Measurement and Calculations*

85   Grain-size distribution is calculated using the refractive index of quartz (1.56) for the

86   sediment and 1.0 for the water. After measurement, the data are saved in a file containing all

87   percentiles and a variety of calculated parameters. Each size class *I* is characterized by an

88   amount noted *T(i)*. The computer software also computes a cumulative and frequency

89   histogram for each sample. The data are transferred to a spreadsheet using a macro that

90   samples the data at increments chosen by the user (in our case, #/6). # (phi) is the negative

91   logarithm to the base 2 of the particle diameter in millimetres.

92

93   *Distribution of the Carbonate Fraction.*

94   The major advantage of a laser diffraction grain-size analyzer is the ability to measure

95   a sediment suspended in water. This allows the addition of the necessary amount of

96   hydrochloric acid (HCl) to dissolve the calcium carbonate contained in the sediment, an

97   approach already used by McCave et al. (1986) to characterize the non carbonate fraction.

98   HCl is added in excess to the suspension, verified by stabilization of the measured pH at a

99   value of 1 for more than one minute. The instrument does not suffer from the acid conditions,

100   because the main parts are made of Teflon, glass, or stainless steel. A repeat measurement is

101   performed after acid digestion to obtain a ''non carbonate fraction'' grain-size distribution.

102   For each size class i, the decarbonated fraction is expressed as $D(i)$.

103   After transferring data to the spreadsheet, the carbonate fraction $C(i)$ is calculated by

104   the formula

105 $$C(i) = T(i) - D(i) \times (1 - CaCO_3) \tag{4}$$

106   derived from McCave et al. (1995b), where $C(i)$ is the calcium carbonate fraction of the size

107   class i, $T(i)$ is the total sediment fraction of size class i, $D(i)$ is the decarbonated sediment

108   fraction of size class i, and $CaCO_3$ is the calcium carbonate content in the sediment, as

109   described next.

110

111   *Calculation of the* $CaCO_3$ *Percentage.*

112   Although it is possible to measure the $CaCO_3$ content by classical chemical

113   techniques, we found that the Malvern Mastersizer was able to calculate automatically the

114   carbonate content of a sediment measured first as a total sediment and then as a decarbonated

115   sediment. Among the different parameters measured by the instrument, ''obscuration''

116   corresponds to the loss of transmitted light intensity due to the presence of particles in

117   suspension. For a monodispersed sample, obscuration is a direct function of grain size,

118   concentration, and path length (width of the measurement cell) according to the following

119   formula

120 $$V = \frac{-d \times \ln(L - O)}{3.1} \tag{2}$$

121   (Malvern Instruments Ltd. Reference manual), where V is the volume concentration as

122   relative percentage, d is the particle diameter in microns, L is the path length illuminated

123   expressed in millimeters, and O is the obscuration.

124   It follows from this relationship that the decrease in concentration between the two

125   grain size measurements (before and after acid digestion) will cause a decrease in the

126   obscuration directly related to the loss of particles dissolved by hydrochloric acid.

127   The $CaCO_3$ content can therefore be directly expressed by the formula

128 $$CaCO_3 = \frac{ObsT - ObsD}{ObsT} \tag{3}$$

129   where $CaCO_3$ is $CaCO_3$ the calcite content, ObsT is the obscuration measured when the total

130   sample is in suspension, and ObsD is the obscuration measured after acid digestion

131   (decarbonated sample).

132   This was tested by measuring the carbonate content both by chemical digestion and by

133   obscuration difference using Equation 3 (Fig. 1). Although the correlation is very good

134   (correlation coefficient $r = 0.9877$), it is notable that the correlation line is not 1:1, indicating

135   that the carbonate content measured with the obscuration difference has to be calibrated to

136   better represent the carbonate content. This is most likely because obscuration also depends

137   on the grain size (Malvern Instruments Ltd., Reference Manual). We therefore suggest that a

138   calibration should be made with samples from each new location.

139   Substitution of Equation 3 into Equation 1 gives

140    $$C(i) = T(i) - D(i) \times \frac{ObsD}{ObsT} \qquad (4)$$

141   Equation 4 facilitates drawing of the cumulative or frequency distribution curve of the

142   carbonate fraction from the sediment, permitting identification of the mode, mean, sorting

143   index, or skewness. Figure 2 illustrates the three curves for a sample from the Northern

144   Atlantic Ocean.

145

146   **Application to pelagic sediments**

147   To test the method on natural samples, we selected 16 samples from the ODP leg 162,

148   site 980, in the Northern Atlantic Ocean, on the western slope of the Rockall Trough at a

149   depth of 2180 m (Jansen et al. 1996). To both emphasize the possible changes in the

150   carbonate fraction of the sediment and to scan a wide variety of $CaCO_3$ content, we used

151   samples dated at the transition between the Pleistocene isotope stages 6 and 5e, between

152   25.26 and 20.56 m below sea floor (146.5 to 119.0 ka, respectively). The sediment consists of

153   calcareous oozes and muds. It is rich in foraminifers of diameter greater than the

154   measurement range. For that reason, it was decided to sieve the sediment at 80 µm very

155   gently under deionized water to remove the large foraminifer fraction. The 16 samples were

156   then prepared as described, and their grain-size distribution was measured on both total and

157   decarbonated fraction.

158   A number of analyses have been performed onboard and in the shore-based

159   laboratory: grain-size distribution, $\delta^{18}O$ composition, and reflectance. Values of mean grain

160   size measured on the bulk sediment range between 6.5 and 20 µm with no trend in the depth

161   distribution (Fig. 3A). After acid digestion (decarbonated sample in Fig. 3A), the usually

162   higher values of the mean grain size indicate that the terrigenous fraction is slightly coarser

163   than the carbonate fraction that is probably rich in nannofossils. The carbonate-fraction mean

164   grain size varies between 4.5 and 16.5μm, with variations similar to those observed in the

165   other fractions. It is clear from Fig. 3A that the grain-size distribution of the bulk sediment in

166   this example is not an informative parameter, even if it is sometimes interesting to illustrate

167   variations in the sediment regime related to climatic change (Wang et al. 1999). The age

168   model has been established from the $\delta^{18}O$ stratigraphy measured on *Cibicides* sp. (Fig. 3B,

169   Jerry McManus, unpublished data). The isotope stage 6–5e transition is especially well

170   pronounced at this location because of its proximity to the polar front in glacial stages but

171   distance from it during interglacial stages. Using the technique described above, $CaCO_3$

172   content ranges from 11.5 to 84% (Fig. 3C). There is a clear increase in carbonate at the

173   transition, interpreted to be related to an increase in carbonate productivity during isotope

174   stage 5e (considering no change in the dissolution conditions (Milliman and Droxler 1996) or

175   winnowing removal of the carbonate (Michels 2000)) with a time lag that can be evaluated as

176   0.3 to 0.4 ka between the change in $\delta^{18}O$ composition and the change in $CaCO_3$. The duration

177   of this interval might be explained, in part, by the sampling interval. Reflectance measured

178   onboard (Fig. 3D, Ortiz et al. 1999), on the contrary, is directly related to C content as

179   observed in numerous oceanic locations (e.g., Blum 1997).

180   The $CaCO_3$ content estimated from the obscuration difference (Equation 3) is used to

181   produce the 16 carbonate grain-size distributions (Fig. 4). The surface of the histograms is

182   directly related to the general carbonate content and emphasizes the climatic transition around

183   130 ka. The carbonate-fraction distribution indicates two modal sizes centred at 2 and 32 μm.

184   Smear-slide observations indicate that these modes correspond to nannofossils and planktonic

185   foraminifers, respectively. During the end of glacial stage 6, there is a clear dominance of

186   nannofossils over foraminifers in most samples. This is not the case during the early part of

187   stage 5e (samples at 130.5 and 126.5 ka) when the foraminifer modal class is of the same

188   order of magnitude as that of the nannofossil, indicating that foraminifers are a major

189   contributor (in volume or in weight) to the $CaCO_3$ sedimentation. After this transition,

190   nannofossil abundance increases rapidly to assume the main mode while the foraminifer

191   mode increases slowly. The reasons for this two-phase transition between the glacial and an

192   interglacial stage are not discussed here but indicate a phase lag that has to be confirmed by

193   studies on other transitions or over a longer time period.

194

195   **Discussion**

196   The technique described has great potential utility, making possible a fast

197   determination of the carbonate content with a good accuracy and yielding the carbonate

198 distribution over the studied grain size range. Nevertheless, there is always a vital need to

199 verify the interpretations by visual observations, especially due to some uncertainties, such as

200 sample quality and instrumental limitations.

201

202 *Sample Quality*

203 Detrital Calcite.—Calcite can be present in oceanic sediments as a contributor to the detrital

204 fraction. Although calcite is easily distinguished on smear slides, the method we describe

205 cannot differentiate between biogenic and detrital calcite. For that reason, we recommend

206 closer examination of some samples to avoid misinterpretations. At site 980 in the Northern

207 Atlantic Ocean, smear-slide observations indicate the absence of such a contribution along the

208 study interval.

209 Diagenetic Calcite.—Grain size analyses can easily be performed on non cemented samples.

210 The technique described here must be applied to sediments that have not suffered from any

211 carbonate diagenesis. None of the present-day existing methods for measuring grain size can

212 make the distinction between diagenetic calcite and biogenic calcite.

213

214 **Instrument Limitations**

215 High Carbonate Content.—The accuracy of the $CaCO_3$ content measurement decreases with

216 increasing carbonate concentration, as indicated by the increased scatter in Figure 1 for values

217 greater than 60%. Equation 3 indicates that carbonate content is directly related to the

218 obscuration parameter. The obscuration values have to fall within the grain-sizer range. The

219 instrument can measure with obscurations that are higher or lower (>30% or <10%,

220 respectively; Malvern instrument Ltd. reference manual) than the optimal case, but there is an

221 associated loss of accuracy.

222   Using these values of obscuration, the maximum carbonate content can be calculated

223 by substituting obscuration values in Equation 3

224

225 $$CaCO_{3\text{Max}} = \frac{Obs_{T\text{Max}} - Pbs_{D\text{Min}}}{Obs_{T\text{Max}}} \times 100 = \frac{30-10}{30} \times 100 = 66.6\% \tag{5}$$

226

227   If a deterioration of the measurement is acceptable (replacing $Obs_{T\text{Max}}$ and $Obs_{D\text{Min}}$ by

228 50 and 5, respectively; Malvern instrument Ltd. reference manual), then a maximum value of

229 90% of carbonate content is obtained using Equation 3. This means that above 66.6% of

230 carbonate, the carbonate content accuracy decreases rapidly to be non-measurable above 90

231 %. ObsT is fixed by the instrument user. It is therefore recommended to introduce a large
232 quantity of bulk sediment when a high carbonate content is expected, to maintain enough
233 material after acid digestion.

234 Low Carbonate Content.—When the carbonate content is too low (approaching 15%), the
235 measurements approach the accuracy limit of the instrument. Note in Figure 1 that the
236 intercept at the origin is not zero, indicating that in the case of very low carbonate
237 concentration a higher volume is calculated. It also indicates that incorporating acid in the
238 sampling cell could affect the grain-size distribution even if no carbonate is present in the
239 sediment.

240 Measurement Accuracy of Carbonate Content.—The two previous sections indicate that in
241 some cases, measurement of carbonate content can suffer from a decrease in analysis
242 accuracy if carbonate content is calculated using obscuration parameters. To avoid this
243 problem, it is more suitable to use data on carbonate content from other methods as acid
244 digestion and use Equation 1. However, this causes extra laboratory work and is slower.
245 Furthermore, some problems can occur because the $CaCO_3$ analysis is not performed on
246 strictly the same sample, leading to a loss of precision in calculating the size distribution of
247 the carbonate fraction.

248

249 **Conclusions**

250 With the ability to measure the concentration and grain size distribution first on total
251 sediment and then on the same, but decarbonated, sample by the laser diffraction size
252 analyzer, we demonstrate that by using simple mathematical formulae and a spreadsheet
253 program it is possible to calculate the carbonate content and the grain size distribution of the
254 carbonate fraction. A first application on samples from the Stage 5e–6 Pleistocene climatic
255 transition in the Northern Atlantic Ocean with variable carbonate content indicates the
256 reliability of the method. Thus, use of a laser diffraction size analyzer can be of great value in
257 paleoceanographic studies. This rapid method must still take into account the sample quality,
258 to avoid mistakes in interpreting the carbonate distribution.

259

268

269 **REFERENCES**

270 AGRAWAL, Y.C., MCCAVE, I.N., AND RILEY, J.B., 1991, Laser diffraction size analysis,
271 *in* Syvitski, J.P.M., ed., Principles, Methods, and Application of Particle Size Analysis:
272 Cambridge, U.K., Cambridge University Press, p. 119–128.

273 BALSAM, W.L., DEATON, B.C., AND DAMUTH, J.E., 1999, Evaluating optical lightness
274 as a proxy for carbonate content in marine sediment cores: Marine Geology, v. 161, p. 141–
275 153.

276 BEUSELINCK, L., GOVERS, G., POESEN, J., DEGRAER, G., AND FROYEN, L., 1998,
277 Grain size analysis by laser diffractometry: comparison with the sieve pipette method: Catena,
278 v. 32, p. 193– 208.

279 BLUM, P., 1997, Physical properties handbook: guide to the shipboard measurement of
280 physical properties of deep-sea cores by the Ocean Drilling Program. Available from World
281 Wide   Web:(http://www-odp.tamu.edu/publications/tnotes/tn26/INDEX.HTM':   ODP
282 Technical Notes, v. 26: College Station, Texas, USA.

283 CLEMENS, S.C., AND PRELL, W.L., 1990, Late Pleistocene variability of Arabian Sea
284 summer monsoon winds and continental aridity: eolian records from the lithogenic
285 component of deep-sea sediments: Paleoceanography, v. 5, p. 109–145.

286 DIEKMANN, B., AND KUHN, G., 1997, Terrigene Partikeltransporte als Abbild
287 spätquartärer Tiefen— und Bodenwasserzirkulation im Südatlantik und angrenzendem
288 Südpolarmeer: Deutsche Geologische Gesellschaft, Zeitschrift, v. 148, p. 405–429.

289 FAUGE`RES, J.C., AND STOW, D.A.W., 1993, Bottom-current-controlled sedimentation: a
290 synthesis of the contourite problem: Sedimentary Geology, v. 82, p. 287–297.

291 JANSEN, E., RAYMO, M.E., BLUM, P., ET AL., 1996, Proceedings of the Ocean Drilling
292 Program, Initial Reports, 162: College Station, Texas.

293 KAIHO, K., 1999, Evolution in the test size of deep-sea benthic foraminifera during the past
294 120 m.y.: Marine Micropaleontology, v. 37, p. 53–65.

295 KENCH, P.S., AND MCLEAN, R.F., 1997, A comparison of settling and sieve techniques
296 for the analysis of bioclastic sediments: Sedimentary Geology, v. 109, p. 111–119.

297   KONERT, M., AND VANDENBERGHE, J., 1997, Comparison of laser grain size analysis

298   with pipette and sieve analysis: a solution for the underestimation of the clay fraction:

299   Sedimentology, v. 44, p. 523–535.

300   LOIZEAU, J.-L., ARBOUILLE, D., SANTIAGO, S., AND VERNET, J.-P., 1994, Evaluation

301   of a wide range laser diffraction grain size analyser for use with sediments: Sedimentology, v.

302   41, p. 353–361.

303   MCCAVE, I.N., BRYANT, R.S., COOK, H.F., AND COUGHANOWR, C.A., 1986,

304   Evaluation of a laser diffraction- size analyser for use with natural sediments: Journal of

305   Sedimentary Petrology, v. 56, p. 561–564.

306   MCCAVE, I.N., MANIGHETTI, B., AND BEVERIDGE, N.A.S., 1995a, Circulation in the

307   glacial North Atlantic inferred from grain size measurements: Nature, v. 374, p. 149–152.

308   MCCAVE, I.N., MANIGHETTI, B., AND ROBINSON, S.G., 1995b, Sortable silt and fine

309   sediment size/ composition slicing: Parameters for palaeocurrent speed and

310   palaeoceanography: Palaeoceanography, v. 10, p. 593–610.

311   MCCAVE, I.N., AND SYVITSKI, J.P.M., 1991, Principles and methods of geological

312   particle size analysis, *in* Syvitski, J.P.M., ed., Principles, Methods, and Application of Particle

313   Size Analysis: Cambridge, U.K., Cambridge University Press, p. 3–21.

314   MICHELS, K.H., 2000, Inferring maximum geostrophic current velocities in the Norwegian–

315   Greenland sea from settling-velocity measurements of sediment surface samples: methods,

316   application, and results: Journal of Sedimentary Research, v. 70, p. 1036–1050.

317   MILLIMAN, J.D., AND DROXLER, A.W., 1996, Neritic and pelagic carbonate

318   sedimentation in the marine environment: ignorance is not a bliss: Geologische Rundschau, v.

319   85, p. 496–504.

320   ORTIZ, J.D., O'CONNELL, S., AND MIX, A., 1999, Spectral reflectance observations from

321   recovered sediments, *in* Raymo, M.E., Jansen, E., Blum, P., and Herbert, T.D., eds.,

322   Proceedings of the Ocean Drilling Program, Scientific Results, 162: College Station, p. 259–

323   264.

324   PRINS, M.A., 1997, Pelagic, hemipelagic and turbidite deposition in the Arabian Sea during

325   the Late Quaternary: Universiteit Utrecht, Faculteit Aardwetenschappen, Mededelingen, v.

326   168, 192 p.

327   PUDSEY, C.J., 1992, Late Quaternary changes in Antarctic bottom water velocity inferred

328   from sediment grain size in the northern Weddel Sea: Marine Geology, v. 107, p. 9–33.

329   REA, D.K., AND HOVAN, S.A., 1995, Grain size distribution and depositional processes of

330   the mineral component of abyssal sediments: lessons from the North Pacific:

331   Paleoceanography, v. 12, p. 251–258.

332   WANG, L., SARNTHEIN, M., ERLENKEUZER, H., GRIMALT, J., GROOTES, P.,

333   HEILIG, S., IVANOVA, E., LIENAST, M., PELEJERO, C., AND PFLAUMANN, U., 1999,

334   East Asian monsoon climate during the late Pleistocene: High resolution sediment records

335   from the South China Sea: Marine Geology, v. 156, p. 254–284.

336

337 **Figure captions**
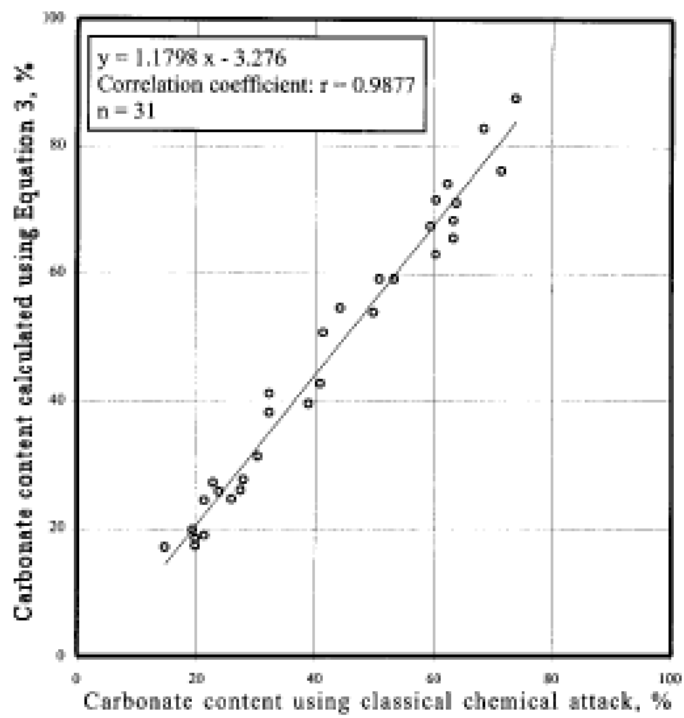
338

339 Fig. 1. Relationship between carbonate content measured by acid digestion and calculated

340 using obscuration parameters on 31 Pleistocene samples from the Northern Atlantic Ocean

341 (ODP Site 980). Values in %.

342

343
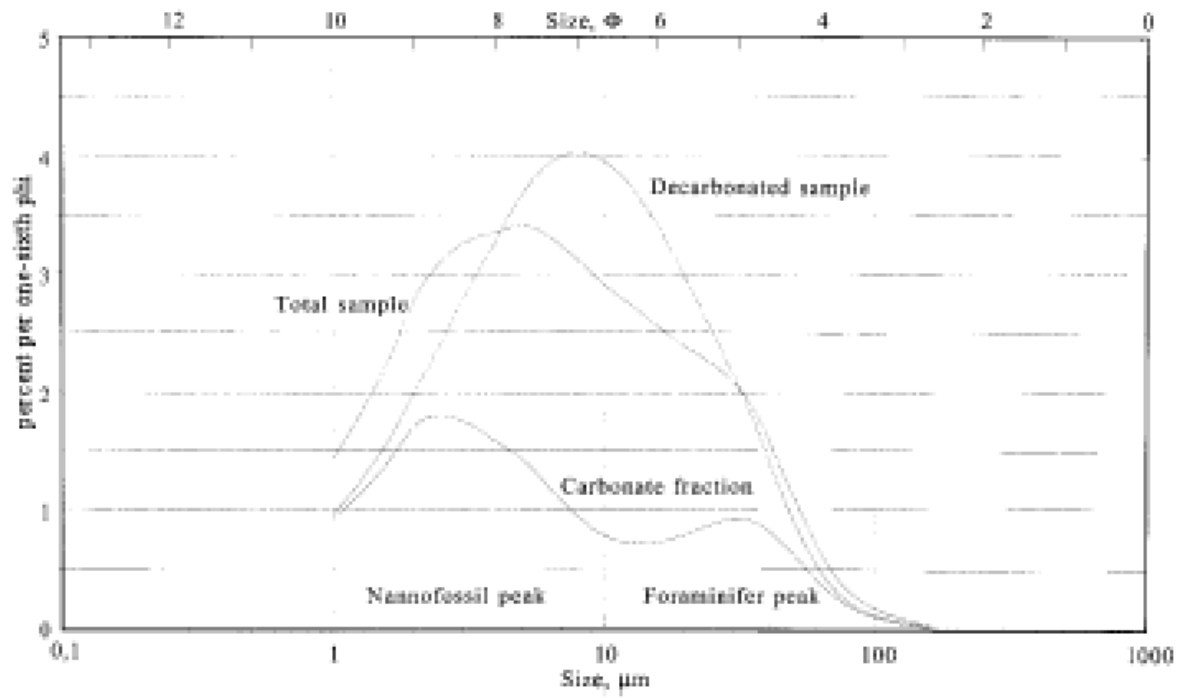
Fig. Grain-size distribution of the sediment before acid digestion (total sediment size distribution: open squares), after acid digestion (decarbonated sediment size distribution: black circles) and calculated carbonate size distribution (carbonate fraction size distribution: black triangles). Sample: 980-C-3H03 016–018, 124.5 ka.
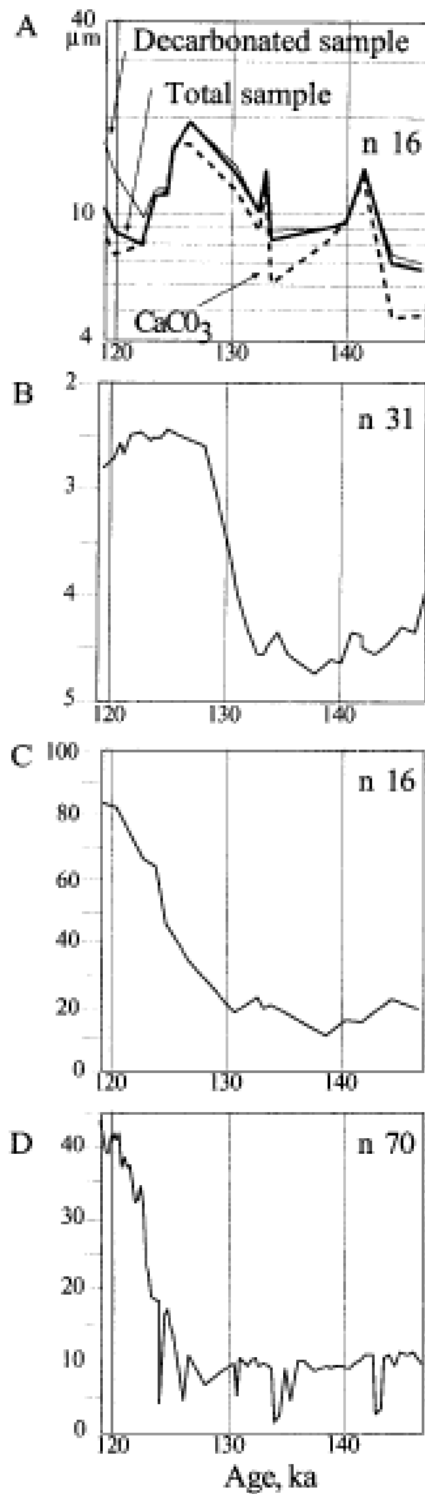
349

350 Fig 3. Variation of different parameters at the transition between the Pleistocene isotope stage

351 6 and 5e. **A)** Mean grain size measured on total sediment, decarbonated sediment, and

352 calculated carbonate fraction; **B)** $\delta^{18}O$ variation (Jerry McManus, unpublished data, in ‰); **C)**

353 $CaCO_3$ content; **D)** Reflectance measured on the red (650 700 nm) band (Ortiz et al. 1999); *n*

354 = number of measurements.

355
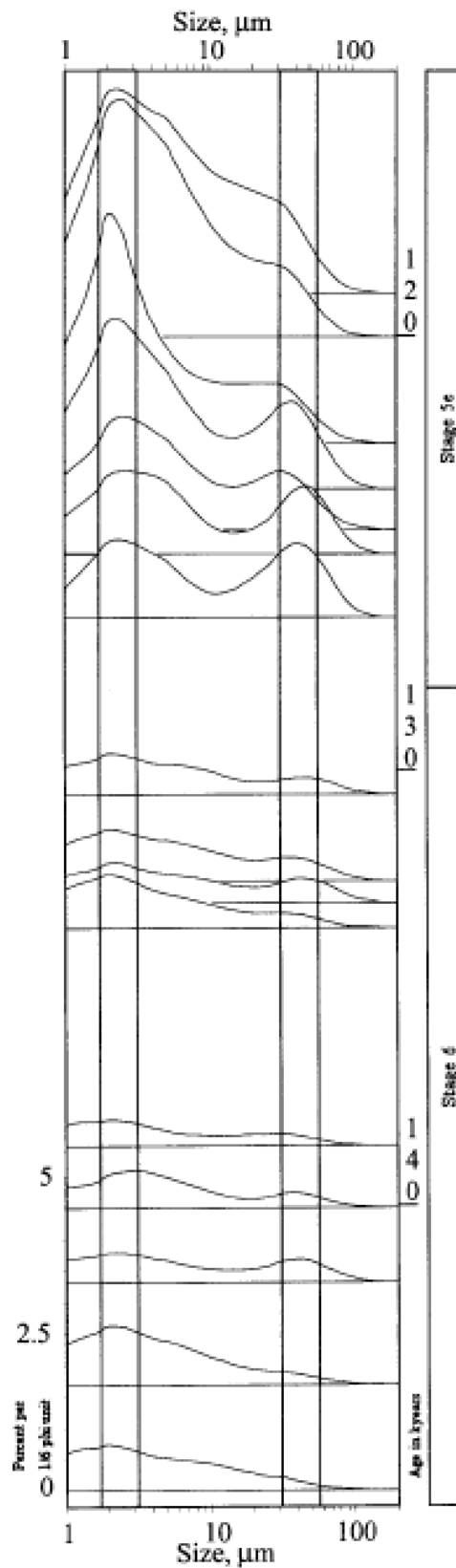
356

357 Fig 4. Grain size distribution of the carbonate fraction in the 16 samples from ODP Site 980.

358 The grey bars located at 2 to 3 microns and 30 to 60 microns represent the two modes,

359 nannofossils and foraminifers.